C-arm CT imaging using the extended line-ellipse-line trajectory: first implementation and initial results

Zijia Guo, Günter Lauritsch, Andreas Maier, Patrick Kugler, Mohammad Islam, Florian Vogt, Frédéric Noo

***Abstract*—In previous work, we proposed a novel data acquisition geometry, called the Extended LEL trajectory, for C-arm CT imaging in interventional radiology. This novel geometry aims at enabling larger axial field-of-view coverage without cone-beam artifacts for imaging with a full X-ray beam as well as with a collimated X-ray beam used for scatter reduction purposes. In this work, we report on a first implementation of the Extended LEL trajectory on a state-of-the-art C-arm system. Highly satisfactory results are shown in terms of trajectory fidelity and repeatability. Suitability of the data for head imaging is also demonstrated using a Rando head phantom without and with 50% beam collimation.**

I. Introduction

C-arm Computed Tomography (CT) is a popular imaging tool in interventional radiology. Currently, the circular short-scan is the preferred data acquisition geometry for C-arm CT. However, the circular short-scan presents two major shortcomings: data incompleteness in terms of Tuy's condition [1], and limited axial coverage. Another important issue that affects image quality is scatter, particularly because the anti-scatter grid used in interventional C-arm systems is suboptimal due to the large variations in source-to-detector distances required by the clinical demands for the system. An alternative option to reduce scatter is axial collimation of the beam, but this further reduces the already limited axial coverage.

To overcome the issues mentioned above, novel data acquisition geometries should be investigated. Recently, we proposed using the Line-Ellipse-Line (LEL) trajectory and its extended version, called the Extended LEL trajectory. This trajectory is designed to provide complete data, as well as extended axial coverage both without and with beam collimation. The Extended LEL trajectory is a continuous curve consisting of tilted ellipses joined together by segments of line. The number of ellipses and the distance separating them define the axial coverage, while the line segments ensure data completeness. The angular tilt applied to the ellipses is critical for image reconstruction at each location from a minimum amount of contiguous projections while allowing uninterrupted data acquisition without double coverage of view positions, as observed with the extended arc-line-arc trajectory [2].

The theoretical properties of the Extended LEL trajectory were thoroughly studied in [3], [4]. Also, experiments from computer simulated data demonstrated accurate image reconstruction with no cone-beam (CB) artifacts and strong robustness to data sampling [3]. In this work, we report on a first implementation of the Extended LEL trajectory on a state-of-the-art C-arm system. The implemented trajectory consists of two ellipses and three lines. The quality of this first implementation was evaluated in terms of geometry fidelity and reproducibility, and also in terms of consistency with theory for CB image reconstruction of an anthropomorphic head phantom without and with beam collimation.

Z. Guo and F. Noo are with the Department of Radiology and Imaging Sciences, University of Utah, USA. G. Lauritsch, P. Kugler and F. Vogt are with Siemens Healthcare GmbH, Germany. A. Maier and Z. Guo are with the University of Erlangen-Nürnberg, Germany. M Islam is with SYNG4 GmbH, Germany.

II. Trajectory Implementation

We implemented the Extended LEL trajectory on a Siemens ARTIS pheno system (Siemens Healthcare, GmbH, Forchheim, Germany), which is a multi-axis robotic floor-mounted C-arm with flat panel detector. The trajectory was pre-defined through the use of 47 control points, using upsampling between the control points to enable data acquisition at 320 positions. The pre-defined trajectory was loaded to the C-arm system via a newly-developed programmable patch. X-ray exposure was triggered by angulations rather than time stamps, to ensure lower impact of motor accelerations and decelerations on geometrical repeatability of measurements.

Technical details regarding the trajectory configuration are listed in Table I. The limited number of projections was due to current software limitations. The relative number of projections between lines and ellipses was based on the requirement of keeping the physical distance between source positions nearly constant. The axial coverage parameters were chosen so as to cover a full head phantom without collimation as well as with a beam collimation of up to 50%.

Source-to-isocenter	$785\ mm$
Source-to-detector	$1300\ mm$
Field-of-view radius	$114\ mm$
Length of each line	$71.6\ mm$
Angular length of each ellipse	210^o
Ellipse-to-ellipse distance	$60\ mm$
Axial tilt of each ellipse	$12\ mm$
Total axial coverage	$192\ mm$
# of control points	47
# of views	320
# of views per ellipse	140-140
# of views per line	13-14-13
Detector pixel size	$0.308 \times 0.308\ mm^2$
Detector size	1248×928

TABLE I: Trajectory configuration

III. Evaluation tests

To assess the quality of the implementation, we performed tests evaluating the fidelity of the geometry and its repeatability, and also tests evaluating the suitability of the data for CB reconstruction of a head phantom.

A. Geometry fidelity and repeatability

The physical position of the source and detector during data acquisition was determined using a geometrical phantom, which we call the PDS-4 phantom. This phantom is specifically designed for calibration of trajectories with large axial coverage. See [5] for details on this phantom. By analyzing each CB projection of the PDS-4 phantom, we obtain full information on the position of the source and the detector relative to the phantom for each location where the X-ray source is triggered.

Geometry fidelity of the data acquisition was performed by comparing the calibrated source positions with the pre-defined trajectory. Geometry repeatability was performed through comparison of source and detector placements from one repetition of the data acquisition to another; the comparison was in terms of accuracy in backprojection for voxels within the field-of-view. The repeatability was assessed over 5 immediate repetitions and also over 3 short-term repetitions. The immediate repetitions amount to immediately repeating the protocol. The short-term repetition includes the utilization of a different protocol prior to repetition of the Extended LEL scan to force the system to recall it from another position. The phantom placement remained unchanged between all scan repetitions to avoid dealing with changes in the world coordinate system, which is attached to the phantom.

B. Image reconstruction

A Rando head phantom was used for this test. The phantom was positioned on a foam holder in such a way that transversal truncation is avoided. Axial positioning of the Extended LEL trajectory was such that the first ellipse was centered on the base of the skull and the second one was centered on the middle of the brain.

Prior to image reconstruction, the projection data was corrected for scatter and beam-hardening, and transformed into line integrals using the conventional log transformation with air scan providing information on the incoming fluence.

Reconstruction was formulated as a penalized least-square optimization problem with the penalty term applied to difference between neighbor voxels. This optimization problem was solved in an iterative manner using the GISTA method [6]. Both quadratic regularization and total variation were considered. The quadratic regularizer was used for its ability to produce results similar to a filtered-backprojection reconstruction, which was previously applied to ideal data [3] and which we plan to apply to real data in the future. Total variation was used to mitigate artifacts due to few view sampling, which could be anticipated to be significant given the limited number of measurements over each ellipse.

To assess the suitability of the implemented trajectory with beam collimation, we performed reconstruction from full projections as well as from axially cropped projections mimicking a 50% collimation of the beam.

All reconstructions were performed on a volume of $270 \times 270 \times 300$ cubic voxels covering the field-of-view with a voxel size of $1\,mm$. The number of iterations was 1000. This number was selected on the basis that the difference between using 2000 versus 1000 iterations was negligible on one test case.

IV. Evaluation results

A. Geometry fidelity

Figure 1 shows the Extended LEL trajectory in a 3-D view, as well as its projections on the (x, y)-plane, on the (x, z)-plane, and on the (y, z)-plane. The pre-defined trajectory is indicated by the solid curve, whereas the real trajectory, acquired from the C-arm, is shown with dots. The pre-defined trajectory was generated by interpolating the control points, and performing afterwards a registration to the real trajectory using the iterative closest point method.

Figure 1 shows strong fidelity in the trajectory shape. The ellipses appear as ellipses with the desired tilt, and the line segments appear fairly linear. Also, the transitions between ellipses and lines essentially occur at the desired places. Small deviations do exist. These are best appreciated using zoom plots.

Figure 2 shows a zoom on the connection between the middle line and the second (top) ellipse, and also shows a zoom on the connection between the top ellipse and the last line segment. The regions for these two zooms are indicated as boxes 1 and 2 in Figure 1. More deviations can be observed for the source positions on the lines than for the source positions on the ellipses, particularly near the transition from line to ellipse. However, the deviations are fairly small, on the order of 2-3 mm, so that we can still say that, overall, the geometry fidelity is highly satisfactory.

B. Geometry repeatability

As mentioned earlier, geometry repeatability was evaluated in terms of backprojection accuracy. For each view and each voxel, we computed the detector position to be used for backprojection and assessed how this position changes from one scan repetition to the next. This change in position was scaled by the CB geometry magnifaction factor to reflect an error near the center of the field-of-view. Our results are shown in Figure 3 in the form of box plots that display, over the views, the mean variation that was observed over the voxels.

For the immediate repetitions, the average backprojection error was less than $0.05\,mm$ for at least 75% of the views. The short-term repeatability had a larger average backprojection error, but this error was still less than $0.15\,mm$ for at least 75% of the views, with errors below $0.4\,mm$ for the outlier views. Compared with the standard circular short-scan, the backprojection error for the Extended LEL trajectory is largely comparable (not shown here) and thus promising for this first implementation.

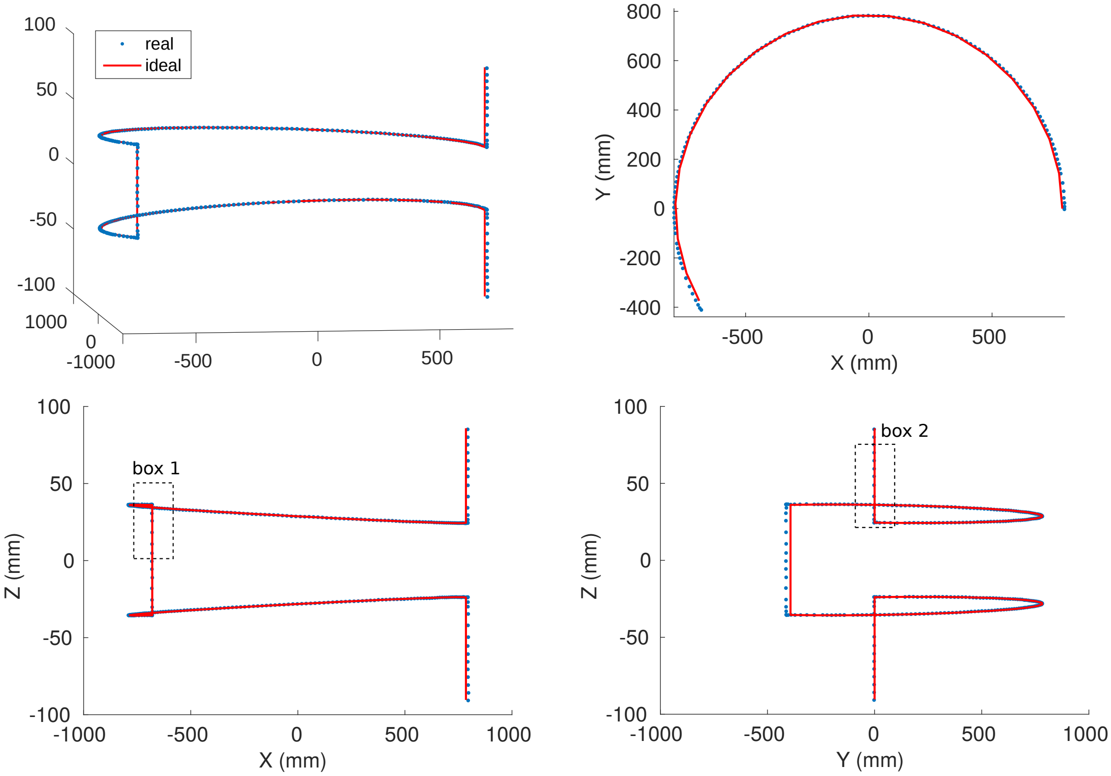

Fig. 1: Plots of the Extended LEL trajectory: 3-D view (top left) and projections on the (x, y)-plane (top right), on the (x, z)-plane (bottom left), and on the (y, z)-plane (bottom right) are shown. The pre-defined trajectory is indicated by the solid curve, whereas the real one, obtained from the C-arm, is shown with dots. All axes are scaled in mm.

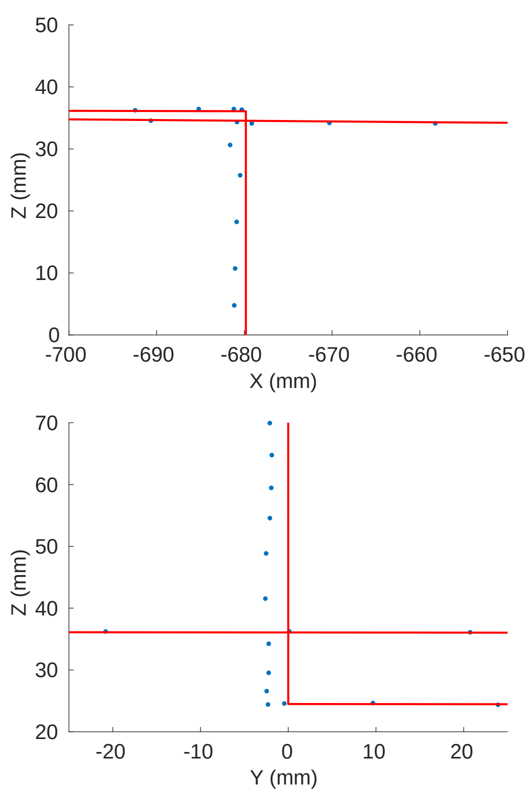

Fig. 2: Zooms on portions of the Extended LEL trajectory indicated as boxes 1 and 2 in Figure 1. All axes are scaled in mm.

C. Image reconstruction

Figure 4 shows a few representative projections along the Extended LEL trajectory. Our first reconstruction of the head phantom showed unexpected artifacts. By inspecting the projection data, we identified that the edges of the collimator cause data inconsistencies that are irrelevant for a circular short-scan reconstruction but matter for the Extended LEL trajectory. After cropping out the inconsistent part from the measurement (about 30 detector rows at both top and bottom of the detector), a much better image quality was obtained. Figure 5 and 6 show the reconstruction with data cropping, using a narrow grayscale window width of 400 HU. Fine details of the bony structures appear clear and no severe CB artifacts are observed. Due to the limited number of projection views and due possibly also to a few select views that showed less repeatability, streak artifacts are observed. As anticipated, more streaks are observed with quadratic regularization than with total variation, which perfoms well at reducing the strength of these streaks.

The data acquisition process with a simulated 50% collimation of the beam is illustrated in Figure 7, and Figure 8 shows reconstructions from this collimated data using the total variation penalty. In this collimated set-up, most voxels are only seen by one ellipse. Although fewer measurements are used for reconstruction, there is no significant difference in noise, primarily because the total variation strength was increased to maintain good mitigation of streak artifacts. This experiment demonstrated that the trajectory still delivered

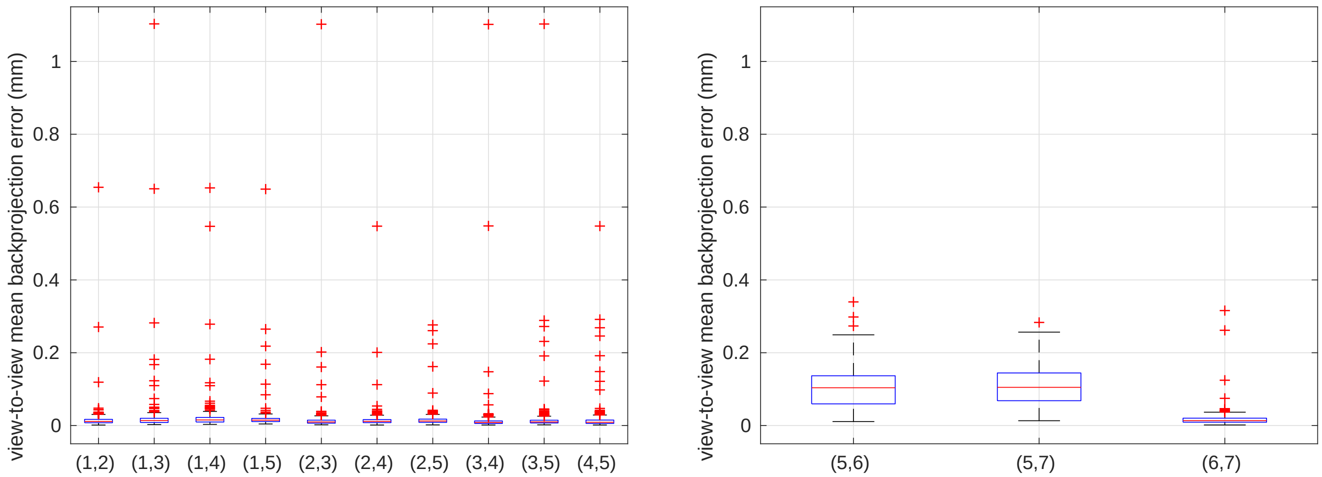

Fig. 3: Box plots showing the view-to-view variations in mean backprojection error over voxels covering the field-of-view, when considering immediate scan repetitions (left) and short-term scan repetitions (right). The horizontal axis indicates the pairs of repeated scans under comparison. The vertical axis shows the distribution of the mean backprojection error over the 320 views. Each box accounts for 75% of the views. The crosses mark outliers.

sufficient data for reconstruction, as anticipated by the theory. (Naturally, the upper and lower portion of the phantom are now truncated.)

V. Conclusion and Discussion

We reported on a successful first implementation of the Extended LEL trajectory on a state-of-the-art C-arm system used in interventional radiology. Promising results were shown in terms of trajectory fidelity, data acquisition repeatability, and data suitability for head imaging. This work demonstrates the feasibility of data acquisition on a C-arm system with a trajectory other than the standard circular short scan for axially extended field-of-view imaging, without and with beam collimation for scatter reduction purposes. Future work will focus on refining the software component to enable the utilization of more projections. Once more projections are available, analytical reconstruction, which would be clinically more practical, will be investigated.

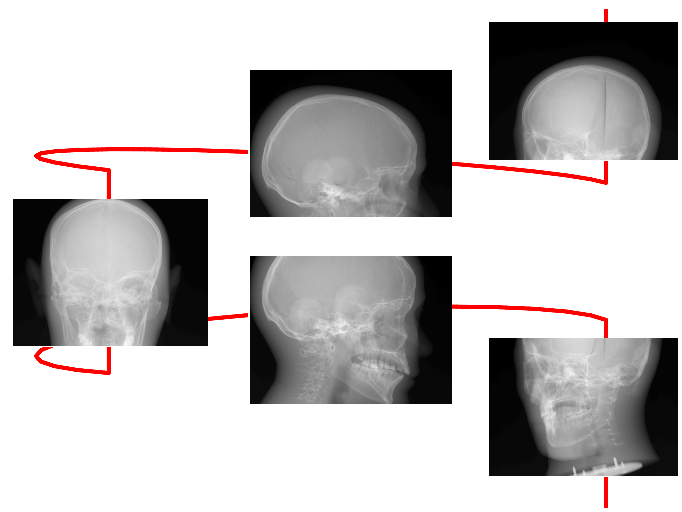

Fig. 4: Illustration of a few representative projections along the Extended LEL trajectory obtained when scanning the Rando head phantom.

Disclaimer

The concepts and information presented in this paper are based on research and are not commercially available.

Acknowledgment

This work was supported by a research contract with Siemens Medical Solutions USA, Inc. This work was also partly supported by the Erlangen Graduate School in Advanced Optical Technologies (SAOT); the authors gratefully acknowledge funding of SAOT by the German Research Foundation (DFG) in the framework of the German excellence initiative.

References

[1] Tuy, H. K., "An inversion formula for cone-beam reconstruction," *SIAM J. Appl. Math.* **43**, 546–552 (June 1983).

[2] Yu, Z., Wunderlich, A., Dennerlein, F., Lauritsch, G., and Noo, F., "Line plus arc source trajectories and their R-line coverage for long-object cone-beam imaging with a C-arm system," *Phys. Med. Biol.* **56**, 3447–3471 (May 2011).

[3] Yu, Z., Noo, F., Lauritsch, G., and Hornegger, J., "Extended-volume image reconstruction using the ellipse-line-ellipse trajectory for a C-arm system," in [*Proceedings of the 12th International Meeting on Fully Three-Dimensional Image Reconstruction in Radiology and Nuclear Medicine*], 245–248 (June 2013).

[4] Guo, Z., Noo, F., Maier, A., and Lauritsch, G., "Properties of the ellipse-line-ellipse trajectory with asymmetrical variations," in [*Medical Imaging 2016: Physics of Medical Imaging*], **9783**, 97832Z, International Society for Optics and Photonics (2016).

[5] Yu, Z., Maier, A., Lauritsch, G., F., V., Schönhorn, M., C., K., Hornegger, J., and Noo, F., "Axially extended-volume C-arm CT using a reverse helical trajectory in the interventional room," *IEEE Trans. Med. Imaging* **34**, 203–215 (Jan 2015).

[6] Loris, I. and Verhoeven, C., "On a generalization of the iterative soft-thresholding algorithm for the case of non-separable penalty," *Inverse Problems* **27**(12), 125007 (2011).

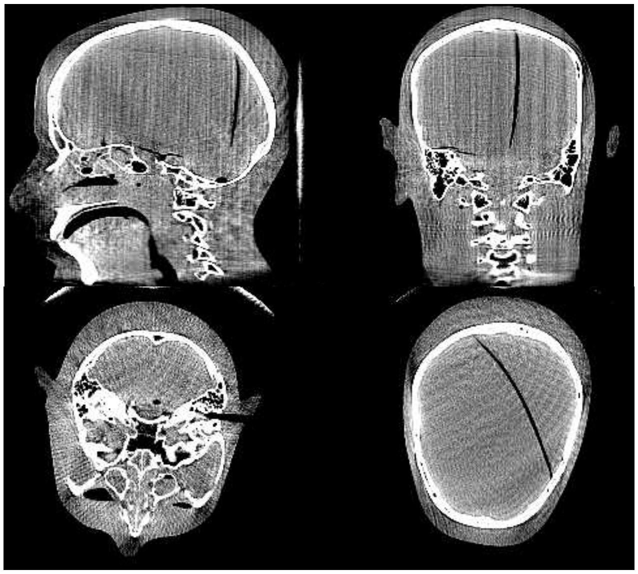

Fig. 5: Reconstruction of the Rando head phantom with quadratic regularization, using all acquired data. Grayscale: $[-200, 200]$ HU.

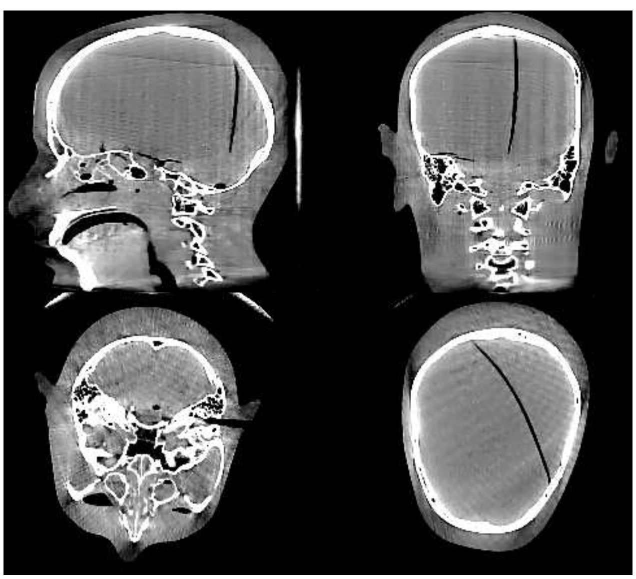

Fig. 6: Reconstruction of the Rando head phantom with total variation regularization, using all acquired data. Grayscale: $[-200, 200]$ HU.

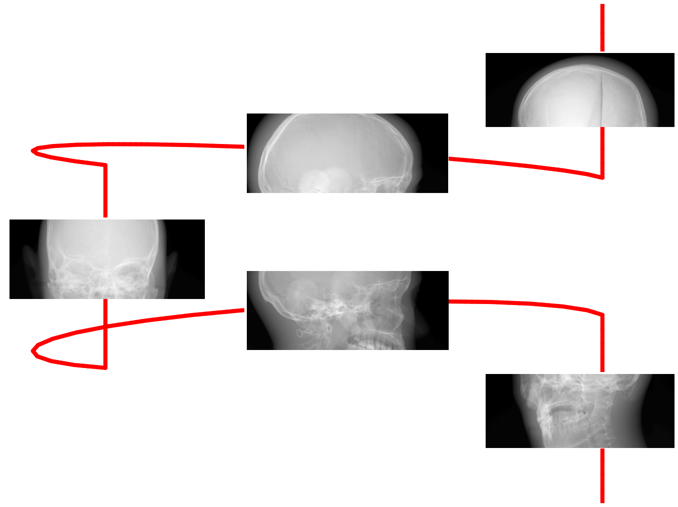

Fig. 7: Illustration of a few representative projections along the Extended LEL trajectory obtained when scanning the Rando head phantom with a simulated 50% collimation of the beam.

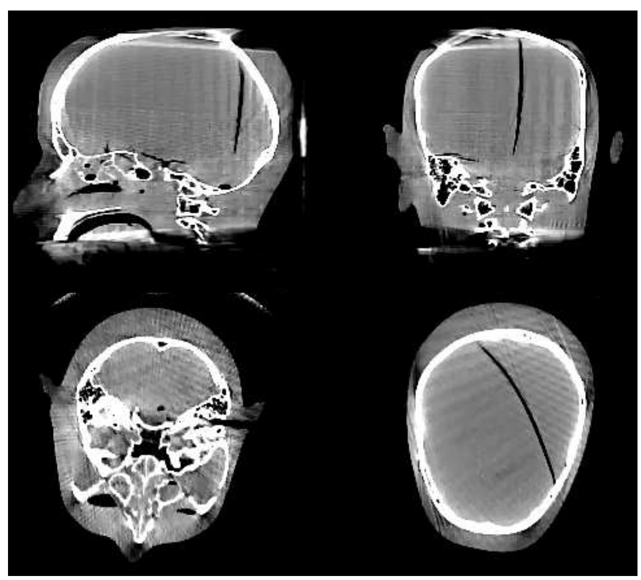

Fig. 8: Reconstruction of the Rando head phantom with total variation regularization, using only the central 50% of the data acquired at each source position, to simulate a 50% beam collimation. Grayscale: $[-200, 200]$ HU.